



Demonstration of an off-axis parabolic receiver for near-range retrieval of lidar ozone profiles

Betsy M. Farris¹, Guillaume P. Gronoff³, William Carrion³, Travis Knepp³, Margaret Pippin²,
Timothy A. Berkoff²

5 ¹Mechanical Engineering, Colorado State University, Fort Collins, CO 80523, USA

²NASA Langley Research Center, Hampton, VA 23681, USA

³Space Systems & Applications, Hampton, VA 23681, USA

Correspondence to: Timothy A. Berkoff (timothy.a.berkoff@nasa.gov)

Abstract.

10 During the 2017 Ozone Water Land Environmental Transition Study (OWLETS), the Langley Mobile Ozone Lidar system utilized a new small diameter receiver to improve the retrieval of near-surface signals from 0.1 to 1 km in altitude. This new receiver utilizes a single 90 degree fiber-coupled, off-axis parabolic mirror resulting in a compact form that is easy to align. The single reflective surface offers the opportunity to easily expand its use to multiple wavelengths for additional measurement channels such as visible wavelength aerosol measurements. This unique
15 added capability allows for near-field analysis of ozone profile concentrations, enabling the study of near-surface pollution dynamics. Results compare performance of the receiver to both ozonesonde and in-situ measurements from a UAV platform, validating the performance of the near-surface ozone retrievals.

1 Introduction

20 Tropospheric ozone is a trace gas regulated by the U.S. Environmental Protection Agency due to its harmful impacts to human health and the environment. Specifically, ground level ozone can causes serious problems for sensitive groups such as children, elderly, or those with respiratory diseases (Federal Register Environmental Protection Agency, 2015). Formed as a secondary pollutant from oxides of nitrogen, volatile organic compounds and photochemical reactions often present in metropolitan and densely populated communities, ozone must be
25 continuously monitored to comply with current air quality regulations designed to protect the public. Knowing the vertical ozone profile distribution allows for insights into boundary layer dynamics, and free troposphere, providing a more complete understanding of surface ozone behavior. Therefore it is desirable to have instruments capable of measuring ozone at the ground level to stratospheric altitudes.

30 The Tropospheric Ozone Lidar Network (TOLNet) was established by NASA to provide needed observations of ozone vertical distribution to better understand pollution dynamics for improving forecast models and satellite retrievals of atmospheric pollutants (Newchurch et al., 2016). The Langley Mobile Ozone Lidar (LMOL), a participating lidar in TOLNet, is a differential absorption lidar system (De Young et al., 2017) that uses a custom pulsed UV laser that generates two wavelengths to obtain vertical profiles of ozone from backscattered light. The system fits into a small
35 mobile trailer and is capable of being operated at remote locations. LMOL has been used in multiple field campaigns (Leblanc et al., 2017; Sullivan et al., 2014; Wang et al., 2017) and provided data for the Ozone Water-Land



Environmental Transition Study (Sullivan et al., 2018, Berkoff et al., 2017) in summer 2017. The OWLETS campaign aimed to evaluate gradients between water and land in coastal regions, and LMOL provided vertical profiles “over water” by stationing the lidar at the mid-point of the Chesapeake Bay Bridge Tunnel system near the mouth of the Chesapeake Bay. In addition to the UV measurements, this system can also transmit 527 nm light for additional measurements of aerosol and cloud profiles.

One of the key challenges for lidar systems, including those in TOLNet, is recovery of the near-range signals closest to the surface where incomplete transit-receiver geometrical overlap, detector saturation, and other non-linear effects impact the ability to correctly process signals. Secondary smaller diameter receivers with a wider field-of-view are often employed co-aligned with the lidar transmit beam to better recover near-range signals, typically using a single focusing lens (Megie, 1985). In this paper, we describe the use of a unique small-diameter (3”) off-axis parabolic (OAP) fiber-coupled mirror configuration to more easily recover LMOL near-range signals. The OAP approach enables closer range capability for the LMOL instrument in a small compact form and unlike traditional refractive elements, and is able to simultaneously measure green and UV wavelengths more easily.

15

2 Design and Description of Setup

In previous campaigns prior to 2017, LMOL used a 30 cm diameter Fresnel lens as its near-field receiver. This arrangement had alignment stability issues, was mechanically cumbersome, and could only monitor UV signals. For far field measurements (>800 m range in altitude) a 40 cm diameter Newtonian telescope was used to collect backscattered light and provided stable results in prior campaigns for both UV and green wavelengths. The configuration for the OWLETS 2017 campaign maintained the same far-field telescope, laser transmitter and optics while using a new near-field receiver consisting of a 7.6 cm diameter, 90 degree OAP with a 7.6cm focal length (Figure 1). A 1 mm core diameter multimode fiber with a 0.5 numerical aperture matching the fast ($F\#=1$) OAP was mounted in an x-y-z positioning stage and aligned to the focus point of the mirror (Figure 2). The fiber core diameter and mirror focal length combination provides a 13.2 mrad full-angle field-of-view, approximately 10 times larger than the existing far-field receiver. Initial fiber alignment of the OAP was done in a laboratory setting using a visible collimated beam verified by an interferometric shear plate to position the fiber launch at the focal point of the OAP. The fiber x-y-z position was also verified using an autocollimator to examine the quality of beam collimation from the mirror when the fiber was back-illuminated. Once positioned, the fiber distance and position did not require any course adjustments in the field. The entire assembly was mounted on a two axis goniometer with the mirror placed looking upward next to the LMOL far-field receiver. The goniometer arrangement allowed for repeatable angular adjustment of the assembly pointing direction for atmospheric alignment to the LMOL transmitted beam. The LMOL transmitted beam is generated by a tunable Ce:LiCAF laser at a 1 kHz pulse repetition rate, with 0.1 mJ/pulse. Pulse-to-pulse wavelength switching is accomplished with rapid tuning the Ce:LiCAF oscillator between 286 and 292 nm

35



across an ozone absorption feature, enabling differential absorption backscatter measurements of ozone as a function of altitude and time to be obtained (De Young et al., 2017).

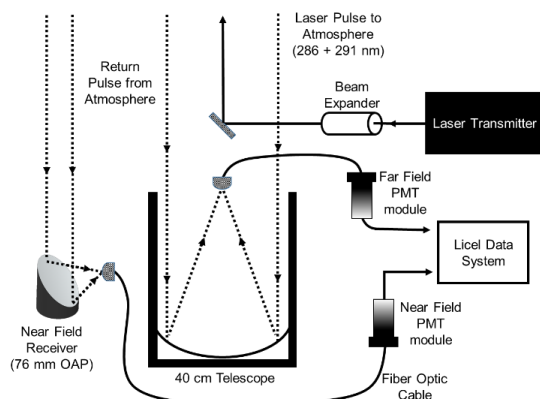


Figure 2: System setup with OAP mirror receiver adjacent to the larger far-field receiver.



Figure 1: Fiber-coupled OAP configuration.

3 Atmospheric Alignment & Measurements

5 The fiber outputs from the near-field and far-field telescopes were coupled to collimating optics, UV bandpass filters (280-295 nm spectral window) that were integrated with Hamamatsu photo-multiplier tube (PMT) detectors in light-tight enclosures. For normal atmospheric science data collection, the outputs of the PMTs were connected to a Licel data system that provided simultaneous analog and photon counting measurements of both the near-field and far-field PMT signals. The Licel system was synchronously gated with the alternating wavelength pulses, so that 286 and 292
10 nm wavelength profiles are separately captured by the data system memory and subsequently recorded to the computer data acquisition system for processing of raw signals into calibrated ozone profiles.

A two-step process is used to align backscattered signals to the near-range and far-range receivers. First, the far-field receiver signal is optimized by changing the angular adjustments on the last outgoing mirror by monitoring the signal
15 on either an oscilloscope or real-time raw signal display generated by the data acquisition system and fixing the mirror in place. The transmitted beam is placed at the center of the far-field receiver FOV, by monitoring the real-time signal amplitude at a range-bin in the upper free troposphere (typically 3-5 km altitude) and centering the mirror adjustments on the maximum signal level. After alignment of the transmitted beam to the far-field receiver, the second step orients the near-field receiver to the transmit beam using the near-field goniometer mount adjustments. The near-field
20 orientation is then optimized by centering its FOV to the transmit beam by finding the center maximum of the signal in the lower free troposphere (typically 1-1.5 km). Because of the higher noise level of the near-field channel, this alignment was refined with a real-time range integrated (ie. 1-1.5 km) signal where sufficient signal could be obtained over a 2-3 second average optimized the near-field receiver alignment. Once both receivers' signals were verified



aligned with the laser beam, then atmospheric data would be collected, typically at 20 second temporally averaged profiles at 7.5 meter vertical sampling resolution.

5 The processing of raw profile signals to obtain calibrated ozone profiles is based on the standard DIAL technique described previously (Browell et al., 1985). Raw signals, both analog and photon counting, are background subtracted and range-squared before applying a single-pass Savitzky-Golay filter. Analog and photon-count channels are merged together to provide a single optimized profile for range and signal-to-noise performance. Ozone cross sections along with pressure and temperature information are used as part of the filter process to extract ozone mixing ratio as a function of altitude. The process is repeated for each new profile on a 5 minute temporal averaged basis, to provide a
10 continuous curtain display on the evolution of ozone vertical distribution during the course of a day.

LMOL far-field ozone profiles prior to 2017 have been compared with ozonesonde launches and other ozone lidar systems in various field campaigns and cross-validation studies (Leblanc et al., 2018; Sullivan et al., 2014). From these investigations, typical cross-comparisons of the far-field channel fall within +/- 5% of the signal level reported, consistent with propagated errors in the LMOL ozone data products.

15 The summer 2017 OWLETS campaign provided a unique opportunity to demonstrate the capabilities of the new near-range OAP receiver for LMOL. The LMOL lidar system was stationed at the third island of the Chesapeake Bay Bridge Tunnel site (CBBT), to obtain “over-water” measurements of ozone. In addition to the lidar, ozonesonde flights were regularly launched from CBBT during the OWLETS campaign. Each ozonesonde flight contained an in-situ instrumentation package consisting of an iMet radiosonde measuring temperature, water vapor, winds, and
20 pressure along with an electrochemical ozone sensor package manufactured by EN-SCI.

The OAP receiver alignment procedure was optimized during the OWLETS campaign and used to retrieve ozone profiles between 120 and 1000 meters in altitude, nearly the entire atmospheric boundary layer. Values below 120
25 meters in altitude were significantly influenced by typical near-range non-linear effects and are screened from analysis in a similar fashion that far-field data is screened from 0-400 meters in altitude. Future development of a similar OAP system for even closer-range capability is being considered.

30 For the OAP performance analysis, OWLETS data taken on Aug 1-2, 2017 represents the most comprehensive inter-comparison opportunity taken during the campaign, with 5 ozonsondes launched during a continuous 32 hour duration of LMOL measurements with the new OAP near-range receiver. In addition, a small drone (UAV) with an in-situ ozone monitor on-board was also flown at this time at the same CBBT location, providing near-range vertical ozone profiles from 0-200 meters in altitude, allowing for additional lidar inter-comparisons on both days. The UAV in-situ ozone sensor consisted of a 2B Technologies model POM device that is an approved Federal Equivalent Method
35 (FEM) and NIST traceable ozone measurement with +/- 2 ppbv or better absolute accuracy, and contained its own built-in data storage, battery, sampling air flow pump, and GPS tracker (2B Technologies, 2016). The POM was



mounted to the top structure of the UAV and then flown in different flight patterns to investigate near-range variability in ozone at the CBBT site.

Figure 3 displays the 32 hour data taken by the near-range OAP receiver, overlaid with the ozonesonde, UAV and surface in-situ ozone measurements taken in the Aug 1-2 time frame. The vertical resolution of the lidar data changes with altitude by an adaptive smoothing technique that is described in work detailing a titration event captured during the OWLETS campaign (Gronoff et al., 2018). Data collection started approximately 8 am local time on Aug 1, with surface and near-surface ozone increasing in magnitude as the day progresses. Collapse of the boundary layer can be seen ~ 20 UTC (4 pm local time) that contributes to the formation of a more defined enhanced ozone layer (up to 95 ppbv) approximately 400 meters above the surface that remains as a residual layer into the evening, possibly contributing to some marginal ozone enhancement at the surface until 4 UTC. Values at the surface and lowest altitudes then decrease significantly in the early morning Aug 1 hours as the elevated layer also somewhat dissipates and also mixes to higher altitudes with the growth of the Aug. 1 boundary layer. This result from the new near-range OAP capability illustrates the temporal evolution of ozone can be complex, and more clearly reveal how near surface ozone layers potential interact with surface ozone levels.

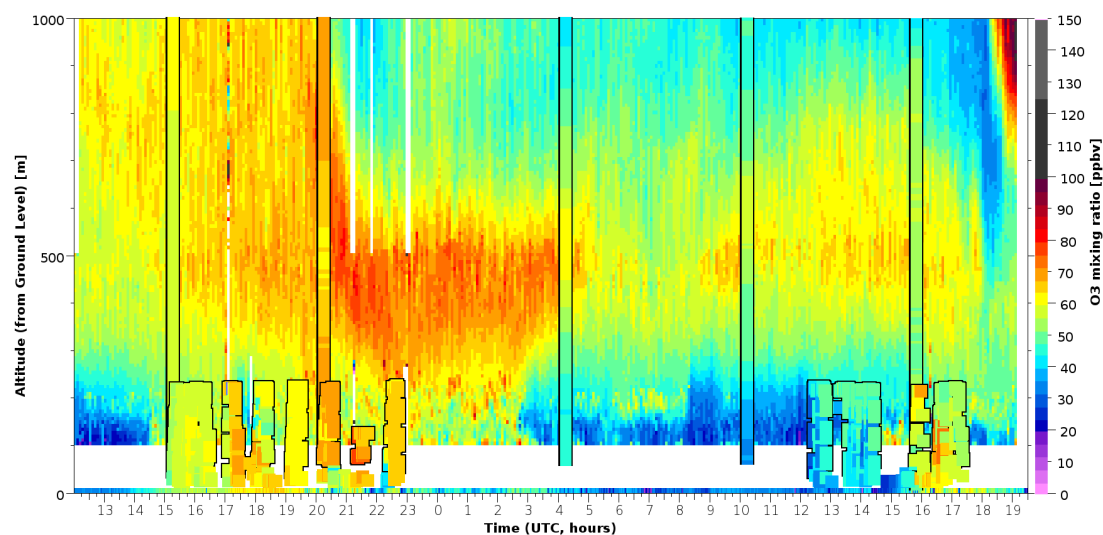


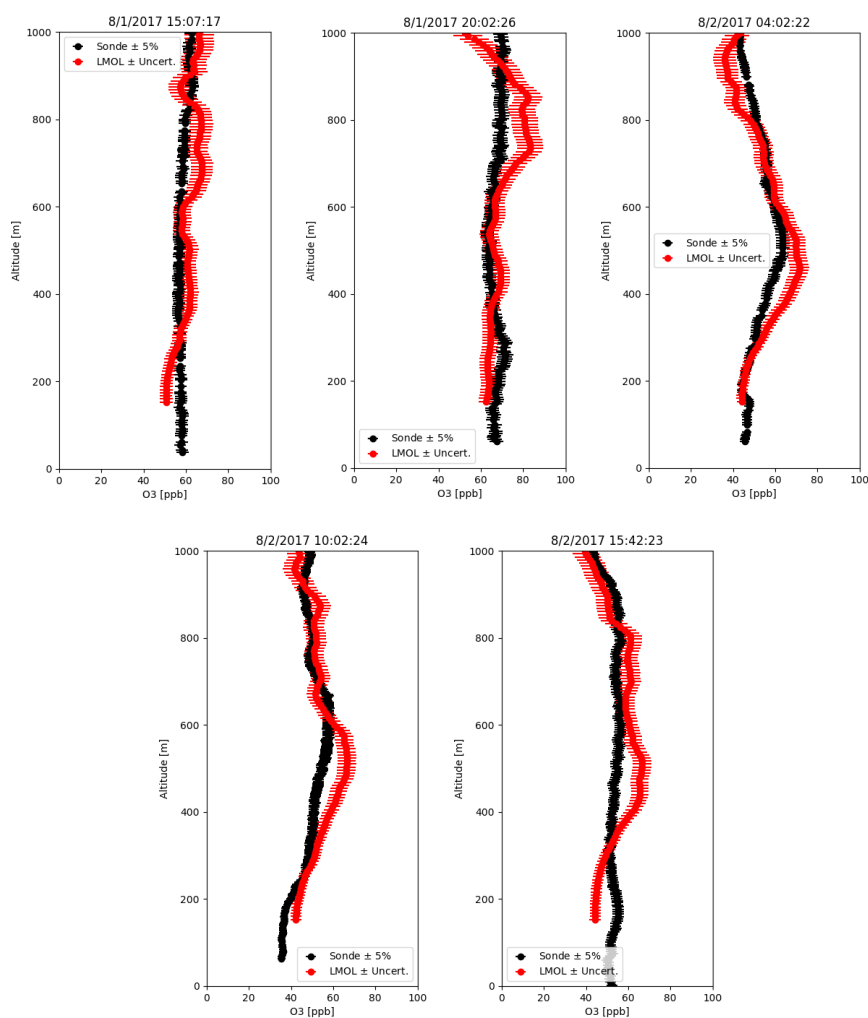
Figure 3: LMOL ozone 32-hour lidar curtain obtained Aug 1-2, overlaid with five ozonesonde measurements and UAV in-situ measurements (0-200 m).

In general, the ozone measurements between lidar, ozonesonde, surface, and UAV were found to be fairly consistent with each other where spatio-temporal coincidences occur. Although differences can occur in ozonesonde-lidar comparisons due to atmospheric sampling discrepancies due to wind advection of the ozonesonde position, as well as



the time constant of the electro-chemical sensor. From discussions with the manufacturer, and known ascent rate of the ozonesonde, vertical resolution of the ozonesonde is estimated to be 200 meters.

Figure 4 shows the ozonesonde profiles and corresponding OAP near-range receiver profiles and the corresponding uncertainties. For this comparison, the OAP receiver data was smoothed to 200 meter resolution to match the expected ozonesonde vertical resolution.



10

Figure 4: Ozonesonde and LMOL comparison for near field (0-1000 m).



	Sonde Mean +/- St. Dev.	LMOL Mean +/- St. Dev.	% Difference
Flight 1 15:00 UTC	58.5 ± 1.97	60.8 ± 4.92	-3.86
Flight 2 20:00 UTC	67.3 ± 2.35	69.5 ± 6.85	-3.22
Flight 3 04:00 UTC	52.7 ± 6.26	54.0 ± 10.8	-2.44
Flight 4 10:00 UTC	49.0 ± 6.13	53.4 ± 7.28	-8.59
Flight 5 15:45 UTC	53.1 ± 2.63	55.3 ± 7.72	-4.06

Table 1: Comparison of sonde and LMOL average ozone values (ppbv) and the percent difference in values. The data sample standard deviations are also shown along with the mean values.

As can be seen from Table 1, the differences between lidar and sonde are relatively small, with means of the all profile differences being 4.43%, with the lidar having an overall high bias relative to the ozonsonde launches.

5

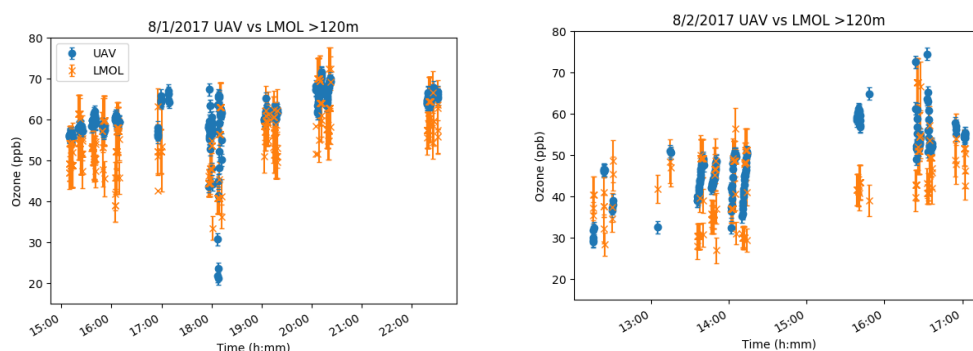


Figure 5: Time Series for 8/1-8/2/2017 of UAV measurements above 120m and the corresponding LMOL data

	UAV Mean +/- St. Dev.	LMOL Mean +/- St. Dev.	% Difference
8/1/2018	60.9 ± 5.92	55.4 ± 7.24	9.46
8/2/2018	48.7 ± 7.76	43.3 ± 8.88	11.63

Table 2: UAV and LMOL comparison for 8/1 and 8/2 for samplings taken above LMOL above 120 m. The data sample standard deviations are also shown along with the mean values.

10

Although the UAV measurements were limited to 200 m altitude due to FAA airspace regulations, a number of vertical profiles were obtained on Aug 1 & 2, and provide additional inter-comparison with the new OAP near-range receiver in the lowest portion of its altitude range. Figure 5 shows a time series comparison during the Aug 1-2 flights over the lidar and within the altitude range of the receiver. Unlike the ozonesonde, the UAV can be held to a controlled fixed position over the lidar, reducing some of the air-mass sampling issues with the ozonesonde. The ozone concentrations measured by the POM on the UAV averaged 9.46 and 11.63% higher than LMOL measurements for 8/1 and 8/2, respectively.

15

Error discussion

20

TOLNet lidar systems have collectively developed rigorous processing algorithms based on Network for the Detection of Atmospheric Composition Change (NDACC) ozone lidar protocols to ensure consistency in O₃ data products and



associated uncertainties between instruments [Leblanc *et al.*, 2016a,b, Leblanc 2018]. The OAP error bars presented in Figure 4 are the errors propagated from these standardized TOLNet/NDACC protocols, and take into account random detector noise as well as other uncertainties including O₃ absorption and Rayleigh cross-sections used in determining concentration values. Comparisons with co-located electro-chemical ozonsonde flights is a traditional approach used to cross-validate with O₃ lidar profiles, typically limited to 5% absolute accuracy. While the sample standard deviations reported in Table 1 are significant compared to the sonde-lidar difference biases, the per flight 0-1 km mean values allow for higher precision < 1 ppbv (< 2%) determinations due to the significant number of samples available in the column. This precision improvement allows for better overall assessment of static bias error between the OAP and corresponding sonde data. All sonde-lidar column bias differences except flight #4 in Table 1 fall within the 5% sonde absolute accuracy limits. The column averaged propagation of errors following standardized TOLNet protocols for these columns varied between 7.7 to 8.4 percent, somewhat larger than the absolute limits of the sonde. Consequently, these residual sonde-lidar differences are less than expected errors (with the exception of flight #4), indicating agreement to the extent possible within performance limits of the sonde and OAP data.

However, the UAV-lidar differences in Table 2 are biased opposite and somewhat larger than the than the expected instrument error. The exact cause of the larger UAV-lidar bias remains unclear but could be potentially be attributed to multiple factors. The UAV in-situ sensor provides high temporal resolution (10 seconds) with a very small volume sample compared to the OAP observed air mass. The high degree of short-term signal variability evidenced by the UAV/OAP Figure 5 time series suggests rapidly changing significant small scale gradients, making the UAV and lidar co-comparison more challenging than anticipated. The near-surface variability is attributed, in part, to large shipping lane traffic adjacent to the CBBT site as well as other factors, as documented in another paper (Gronoff *et al.*, 2018) where large changes in Pandora columnar NO₂ correlated with lidar near-surface ozone titration events. Furthermore, the signal closest in range have the greatest potential for instrumental error, and limited height range of the UAV may have revealed an increased error for the lowest few recoverable range bins <200 meters, and suggests the need for further investigation. A more detailed study under more stable atmospheric conditions would be needed to more effectively resolve the residual instrumental biases reported here.

4 Summary

It was determined that the improved receiver setup for LMOL allowed for preliminary validation of ozone lidar measurements at a minimum of 120 m compared to the 800 m minimum of the larger far-field receiver. This improvement significantly enhances the capability of the LMOL system allowing for a better understanding of low altitude (120-1000 m) ozone atmospheric dynamics that are critical in evaluating atmospheric models and air pollution satellite retrievals. The new fiber-coupled OAP receiver offers the benefit of small compact form, and can be adapted more easily to aerosol visible wavelength measurements due use of a reflective focusing element. Such a measurement can be possible by using a dichroic beam-splitter at the fiber output to separate green backscattered light from the laser pump of the current system to measure the light separately from the UV retrieval. Comparison measurements with ozonsonde and UAV measurements show good agreement with the ozone values obtained from the new receiver.



LMOL values were biased above the ozonesonde measurements but biased below the UAV measurements, demonstrating reasonable agreement. This new measurement capability for LMOL improvements will continue to further the goals of TOLNet, allowing for development of more compact lower-cost lidar systems with near-range measurement capabilities.

5

Data Availability All data for the OWLETS campaign is publically available at the campaign's website, <https://www-air.larc.nasa.gov/missions/owlets/index.html>

Acknowledgements:

10 This work was supported in part by the NASA Science Innovation Fund, NASA Tropospheric Composition Program, the TEMPO Student Collaboration project with funding provided through the NASA Science Mission Directorate Earth System Science Pathfinder program. Special thanks to an exceptional group of student interns that provided support that made ozonesonde and UAV measurements possible during OWLETS: Lance Nino, Lindsey Rodio, Jeremy Schroeder, Pablo Sanchez, Emily Gargulinski, Marlia Harnden, Desorae Davis, and Angela Atwater. Thanks to
15 Danette Allen, Eddie Adcock, Zak Johns, Mark Motter, Jim Neilan, and Matt Vaughan of the NASA LaRC UAV team. This work could also not have been completed without the helpful accommodations of Edward Spencer and the management and employees with the Chesapeake Bay Bridge and Tunnel District.

20

References:

- 2B Technologies: POM, personal ozone monitor., 1(303), 5–7 [online] Available from:
<http://www.twobtech.com/pom-personal-ozone-monitor.html>, 2016.
- Berkoff, T., Sullivan, J., Pippin, M. R., Gronoff, G., Knepp, T. N., Twigg, L. W., Schroeder, J., Carrion, W., Farris, B., Kowalewski, M. G., Nino, L., Gargulinski, E., Langley, U., Rodio, L., Sanchez, P., Davis, A. A. D., Janz, S. J., Judd, L., Pusede, S., Wolfe, G. M., Stauffer, R. M., Munyan, J., Flynn, J., Moore, B., Dreessen, J., Salkovitz, D., Stumpf, K., King, B., Hanisco, T. F., Brandt, J., Blake, D. R., Abuhassan, N., Cede, A., Tzortziou, M., Demoz, B., Tsay, S.-C., Swap, R., Holben, B. N., Szykman, J., McGee, T. J., Neilan, J. and Allen, D.: Overview of the Ozone Water-Land Environmental Transition Study: Summary of Observations and Initial Results, in American Geophysical Union, Fall Meeting 2017, American Geophysical Union, Fall Meeting 2017, New Orleans, LA. [online] Available from: <https://agu.confex.com/agu/fm17/meetingapp.cgi/Paper/246428>, 2017.
- Browell, E. V, Ismail, S. and Shipley, S. T.: Ultraviolet DIAL measurements of O₃ profiles in regions of spatially inhomogeneous aerosols., *Appl. Opt.*, 24(17), 2827–36, doi:10.1364/AO.24.002827, 1985.
- Federal Register Environmental Protection Agency: National Ambient Air Quality Standards for Ozone Final Rule, 40 CFR Parts 50,51,52,53 58, 80(206), 1–7 [online] Available from:
<https://www.federalregister.gov/documents/2015/10/26/2015-26594/national-ambient-air-quality-standards-for-ozone>, 2015.
- 30
- 35



- Gronoff, G., et al : A Method for Observing Near Range Point Source Induced O₃ Titration Events Using Co-located Lidar and PANDORA measurements, Submitted to Atmospheric Environment, 2018.
- Leblanc, T., Brewer, M. A., Wang, P. S., Granados-Munoz, M. J., Strawbridge, K. B., Travis, M., Firanski, B., Sullivan, J. T., McGee, T. J., Sumnicht, G. K., Twigg, L. W., Berkoff, T. A., Carrion, W., Gronoff, G., Aknan, A., Chen, G., Alvarez, R. J., Langford, A. O., Senff, C. J., Kirgis, G., Johnson, M. S., Kuang, S., and Newchurch, M. J.: Validation of the TOLNet Lidars: The Southern California Ozone Observation Project (SCOOP), Atmos. Meas. Tech. Discuss., <https://doi.org/10.5194/amt-2018-240>, in review, 2018.
- Leblanc, T., Sica, R. J., van Gijsel, J. A. E., Godin-Beekmann, S., Haeefe, A., Trickl, T., Payen, G. and Liberti, G.: Proposed standardized definitions for vertical resolution and uncertainty in the NDACC lidar ozone and temperature algorithms – Part 2: Ozone DIAL uncertainty budget, Atmos. Meas. Tech., 9(8), 4051–4078, doi:10.5194/amt-9-4051-2016, 2016.
- Leblanc, T., Senff, C. J., Sullivan, J., Berkoff, T., Gronoff, G., Strawbridge, K. B., Portafaix, T., Dufлот, V. and Mcgee, T. J.: Using a Centralized Lidar Data Processing Algorithm As a Reference Transfer for the Intercomparison of Campaign Data: Examples from the TOLNet SCOOP and the NDACC MORGANE Campaigns, in American Meteorological Society, 97th Annual Meeting, Seattle, WA. [online] Available from: https://ams.confex.com/ams/97Annual/video gateway.cgi/id/36928?recordingid=36928&uniqueid=Paper310453&entry_password=327228, 2017.
- Megie, G.: Laser Remote Sensing: Fundamentals and Applications, Eos, Trans. Am. Geophys. Union, 66(40), 686, doi:10.1029/EO066i040p00686-05, 1985.
- Newchurch, M., Saadi, J. A. Al, Alvarez, R. J., Burris, J., Cantrell, W., Chen, G., Deyoung, R., Hardesty, R. M., Hoff, R. M., Kaye, J. A., Kuang, S., Langford, A., Leblanc, T., Mcdermid, S., Mcgee, T. J., Pierce, R. B., Senff, C. J., Sullivan, J., Szykman, J., Tonnesen, G. and Wang, L.: Tropospheric Ozone Lidar Network (TOLNet) - Long-term Tropospheric Ozone and Aerosol Profiling for Satellite Continuity and Process Studies, EPJ Web Conf., 119, 20001, 4, doi:<https://doi.org/10.1051/epjconf/201611920001>, 2016.
- Sullivan, J.T, et al. The Ozone Water-Land Environmental Transition Study (OWLETS): An Innovative Strategy for Understanding Chesapeake Bay Pollution Events, Bulletin of the American Meteorological Society, submitted.
- Sullivan, J. T., McGee, T. J., Sumnicht, G. K., Twigg, L. W. and Hoff, R. M.: A mobile differential absorption lidar to measure sub-hourly fluctuation of tropospheric ozone profiles in the Baltimore-Washington, D.C. region, Atmos. Meas. Tech., 7(10), 3529–3548, doi:10.5194/amt-7-3529-2014, 2014.
- Wang, L., Newchurch, M. J., Alvarez, R. J., Berkoff, T. A., Brown, S. S., Carrion, W., De Young, R. J., Johnson, B. J., Ganoë, R., Gronoff, G., Kirgis, G., Kuang, S., Langford, A. O., Leblanc, T., McDuffie, E. E., McGee, T. J., Pliutau, D., Senff, C. J., Sullivan, J. T., Sumnicht, G., Twigg, L. W. and Weinheimer, A. J.: Quantifying TOLNet ozone lidar accuracy during the 2014 DISCOVER-AQ and FRAPPÉ campaigns, Atmos. Meas. Tech., 10(10), 3865–3876, doi:10.5194/amt-10-3865-2017, 2017.
- De Young, R., Carrion, W., Ganoë, R., Pliutau, D., Gronoff, G., Berkoff, T. and Kuang, S.: Langley mobile ozone lidar: ozone and aerosol atmospheric profiling for air quality research, Appl. Opt., 56(3), 721–730,



doi:10.1364/AO.56.000721, 2017.

Zhang, Y., Yi, F., Kong, W. and Yi, Y.: Slope characterization in combining analog and photon count data from atmospheric lidar measurements, *Appl. Opt.*, 53(31), 7312, doi:10.1364/AO.53.007312, 2014.